Reliability Improvements for In-Wheel Motor

Gašper Petelin, Rok Hribar, Stanko Ciglarič, Jernej Herman, Anton Biasizzo, Peter Korošec and Gregor Papa

Abstract Setting up a reliable electric propulsion system in the automotive sector requires an intelligent condition monitoring device capable of reliably assessing the state and the health of the electric motor. To allow for a massive integration of such monitoring devices, they must be inexpensive and small. These requirements limit their accuracy. However, we show in this paper that these limitations can be significantly reduced by appropriate processing of the sensor data. We have used machine learning models (Random Forest and XGBoost) to transform very noisy motor winding insulation resistance measurements made by a low-cost device into a much more reliable value that can compete with measurements made by a high-priced state-of-the-art measurement system. The proposed method is an important building block for a future smart condition monitoring system and enables a cost-effective and accurate assessment of the condition of electric motor health in connection with the condition of their winding insulation.

Key words: In-wheel motor, State of health, Machine learning

1 Introduction

The ongoing developments in road transport and the automotive industry are enabling the introduction of new technologies, such as in-wheel propulsion systems. In addition to changing design and control capabilities and requirements, there is also a demand for increased durability and overall reliability at the system level.

Gašper Petelin, Rok Hribar, Anton Biasizzo, Peter Korošec and Gregor Papa
Jožef Stefan Institute, Slovenia, e-mail: gregor.papa@ijs.si

Gašper Petelin and Rok Hribar
Jožef Stefan International Postgraduate School, Slovenia,

Stanko Ciglarič and Jernej Herman
Elaphe Propulsion Technologies Ltd. e-mail: jernej.herman@elaphe-ev.com

For the in-wheel electric motor system to be widely used in electric vehicles, we need to prove its reliability and introduce some technologies to further improve the reliability and safety of the system by developing an intelligent (smart) condition monitoring system that would increase the reliability of a wheel-integrated solution.

Based on data analysis performed with artificial intelligence (AI) algorithms, we can identify the critical parameters that affect the durability of the engines. This serves as input for a predictive condition monitoring system that can be used in further applications, if possible with self-healing algorithms.

This will support the further deployment of the innovative in-wheel technology by enhancing the system with an intelligent condition monitoring module that uses state-of-the-art AI approaches to detect critical situations, perform predictive analytics and improve overall durability.

The core of the intelligent condition monitoring system is the measuring device for the critical parameters. In order to have a small and cost-effective measuring device, a customized device was developed that allows massive integration into the vehicles. Although such a device is not state of the art in terms of accuracy, we show in this paper that this accuracy gap can be closed and the accuracy of the device can be significantly improved by using appropriate AI-assisted signal processing. By using such a methodology, the measuring device is small and inexpensive, yet fully reliable and accurate.

Before the intelligent condition monitoring system can be used, it is necessary to familiarize with the physics of insulation aging and understand the failure mechanisms and failure modes behind insulation aging (and/or use AI methods instead). This was done through extensive measurements with a series of electric motors as test objects (i.e., device under test-DUT).

The aim is to evaluate the performance of our custom-built Insulation condition monitoring device (ICM) in comparison to the commercially available Metrel device, which serves as the reference measurement standard in our described scenario. This research was conducted as part of the ECSEL JU project iRel40 [1]. The rest of this paper is structured as follows: Section 2 provides a brief overview of the in-wheel electric motor and the associated measurement tools are outlined in Section 3; in Section 4 we present the regression-based prediction techniques; Section 5 presents our experiments and results; and finally Section 6 provides a summary of our study and points out possible future research directions.

2 In-wheel motor

In-wheel electric motors (built into the driven wheels of the vehicle) are an interesting alternative to the traditional e-axle approach for electric propulsion in electric vehicles (one motor per axle, using differential). An electric vehicle with in-wheel motors usually has two (2WD) or four motors (4WD). The in-wheel propulsion offers a number of benefits and certain additional functionalities.

The obvious benefits of direct drive in-wheel propulsion system are:

1. Allows many more free vehicle design options;
2. Simpler construction, with a smaller number of assembly parts, which not only affects the bill of materials and assembly costs, but also reliability;
3. It does not require gearboxes or differentials (therefore no energy losses in these parts – allowing for better energy efficiency);
4. As the torque of each wheel is controlled independently, it also allows torque vectoring - directing torque to a specific wheel where the torque is needed, e.g. more torque is transferred to the outer wheel when cornering;
5. Lower center of gravity;
6. Torque can be controlled at a much higher frequency – thanks to the direct drive;
7. It also enables certain other functionalities that are not possible with other types of propulsion systems.

3 Description of the measurement devices

The device under test is an Elaphe L1500 liquid-cooled outer rotor synchronous motor with permanent magnets, which is designed as an in-wheel solution for electric vehicle drives and is intended for direct- drive applications with high torque requirements [2]. The winding is optimized for a wide operating range in terms of efficiency and speed of typical applications. For voltages different than nominal voltage, the operating range is scaled proportionally to the increase or decrease of the voltage in relation to the nominal voltage of the respective winding configuration. For voltages different than nominal, the speed of the motor increases or decreases accordingly. The basic specifications of the Elaphe L1500 motor can be found in the Table 1 [3].

Table 1 Elaphe L1500 motor specifications.

Nominal supply voltage [V_{DC}]	370
Supply voltage [V_{DC}]	200 - 800
Max torque[1][Nm]	1500
Max speed[2][rpm]	1500

[1] At 200 rpm.
[2] With field weakening, 270 Nm load, and nominal supply voltage.

The winding insulation (i.e., its state of health) protects the motor against short circuits between the motor winding and housing (when integrated into vehicle chassis) and its quality is one of the most important parameters of the electric motor. The quality of the insulation is assessed by various insulation tests.

- Insulation Resistance (IR) measurement is the simplest insulation test. IR is notably high which makes it challenging to measure. After the test connections

have been made, the test voltage is applied for a certain period of time (e.g., 1 min). The total leakage current should drop and remain steady during this period. One can determine the acceptable values for the IR value from experience by measuring the IR value on electric motors in operation. The normal IRs are in the order of Giga Ohms, and the acceptable values reach down to the order of hundreds of mega Ohms.
- Dielectric Absorption Ratio (DAR) measurement is a more reliable insulation test. Good insulation shows an increasing IR value after the test voltage is applied. After the test connections have been made, the test voltage is applied and IR is measured at two different times (e.g., after 0.5 min and after 1 min). The quotient of the latter and the earlier IR measurement is DAR.

3.1 Metrel device

Since the insulation resistance is in the giga-ohm range, the insulation leakage current is very low and therefore difficult to measure accurately. In order to increase the measurement accuracy, high-voltage sources are used with megaohmmeters. In our study, a Metrel megaohmmeter was used to measure insulation resistance and dielectric absorption ratio. Although megohmmeters provide accurate results, their cost is relatively high and special test equipment must be provided, making them difficult to integrate into the vehicle.

Table 2 Metrel measurements and their description (variables stored in Metrel data)

Measurements	Description
Chamber temperature [°C]	Temperature in the chamber at the time of the measurement.
Chamber humidity [%]	Humidity in the chamber at the time of the measurement.
Motor temperature [°C]	Motor temperature at the time of the measurement.
Time [date]	Date/time of the measurement.
Ravg [GOhm]	Average measured resistance

Table 2 lists the measurement attributes of the Metrel device. Chamber temperature, humidity and motor temperature are measured with parallel acquisition systems and data are merged with insulation resistance data acquired by Metrel. They consist of the temperature and humidity in the chamber at the time of measurement, the motor temperature, the time stamp and the average measured resistance in GOhm.

3.2 ICM device

A low-cost impedance measurement circuit (i.e., ICM) was developed to monitor the insulation impedance. It is based on the high-precision impedance transformer system AD5934 [4]. The AD5934 consists of a frequency generator, a 12-bit analog-to-digital converter (ADC), a discrete Fourier transform (DFT) and an I^2C communication interface. The frequency generator is a voltage source used to excite the insulation impedance at known frequencies. The receiver stage of the AD5934 receives the current from the insulation impedance. It consists of an adjustable current-voltage amplifier, a programmable gain amplifier, an anti-aliasing filter and a 12-bit ADC. The digital data from the ADC is passed to the DSP core and a DFT is calculated for each frequency. The results are forwarded to the microcontroller via the I^2C interface. To extend the accurate impedance measurement to higher impedance [5], the voltage source is smoothed and boosted by a low-pass 2^{nd} degree Butterworth filter with a gain of 1.5 and a cut-off frequency of 1.5 kHz. Similarly, the current-voltage amplifier and the signal amplifier are added on the receiving side to improve the sensitivity.

To measure the unknown impedance, the system is first calibrated with a known resistance. A gain is determined from a known resistance and a measured value of the signal at a certain frequency. The unknown impedance is then determined from the calculated gain and the magnitude of the unknown impedance signal at the same frequency. Similarly, the phase is determined from the phases of the measurements of the calibration resistor and the unknown impedance.

Although the resistance measuring range of the developed circuit is at the limit of the insulation resistance range, its cost is significantly lower than the cost of more precise megohmmeters. It can also be integrated into the vehicle, which enables continuous monitoring.

In Table 3 the measurement properties of the ICM device are presented. Similar to the Metrel measurements, details such as the temperature and humidity in the chamber during the measurement, the time stamp and the motor temperature are also documented here. In addition, the resistance, capacitance and dissipation factor are measured at three different frequencies: 1, 1.5 and 2 Hz.

3.3 Testing session

Two motors are simultaneously tested for durability in the Elaphe environmental chamber with controlled temperature and humidity. The motors are placed in a back-to-back pair configuration, with one motor acting as the drive and the other as the load (braking – role of a generator), and vice versa (Fig. 4). In this way, almost all losses are regenerated and fed back into the electric grid.

To accelerate the aging process of the motors, they are subjected to two different cycles: one runs at an approximate chamber temperature of -30 °C, the other at around 85 °C.

Table 3 ICM measurements and their description (variables stored in ICM data)

Measurements	Description
Chamber temperature [°C]	Temperature in the chamber at the time of the measurement.
Chamber humidity [%]	Humidity in the chamber at the time of the measurement.
Motor temperature [°C]	Motor temperature at the time of the measurement.
Time [date]	Date/time of the measurement.
Resistance 1 Hz [MOhm]	Measured resistance at 1 Hz
Resistance 1.5 Hz [MOhm]	Measured resistance at 1.5 Hz
Resistance 2 Hz [MOhm]	Measured resistance at 2 Hz
Capacitance 1 Hz [nF]	Measured capacitance at 1 Hz
Capacitance 1.5 Hz [nF]	Measured capacitance at 1.5 Hz
Capacitance 2 Hz [nF]	Measured capacitance at 2 Hz
Dissipation factor 1 Hz	Measured dissipation factor at 1 Hz
Dissipation factor 1.5 Hz	Measured dissipation factor at 1.5 Hz
Dissipation factor 2 Hz	Measured dissipation factor at 2 Hz

The representative real usage profiles (load profiles) are used in order to obtain data that is as realistic as possible. In our case baseline presented WLTP (World harmonized Lightduty vehicles Test Procedure) driving cycles [6] scaled to higher loads to accelerate insulation aging mechanism.

Each test lasts 30 minutes. The main task is to take a series of measurements after each test cycle to determine whether a winding insulation failure or other fault has occurred. The insulation condition is recorded by both Metrel MI 3205 and Elaphe ICM measuring devices.

The thermal load cycle with the parameters of the two in-wheel motors during complete test session is shown in Figure 2. The test session consists of cold and hot operating cycles with a total duration of 5 h 30 min. The temperature profile on the motor winding during the test cycles is depicted in Figure 3.

4 Predictive algorithm

Both the Metrel and ICM measurements show considerable noise levels. Due to temperature influences, their values can vary by several orders of magnitude, as shown in Fig.4 for the Metrel example. If we only examine the resistance, there is no discernible correlation between the Metrel and ICM measurements due to the aforementioned noise, as can be seen in Fig.5. However, as we show below, by including additional features recognized by the ICM, it is possible to predict the resistance measured by Metrel with satisfactory precision using machine learning techniques.

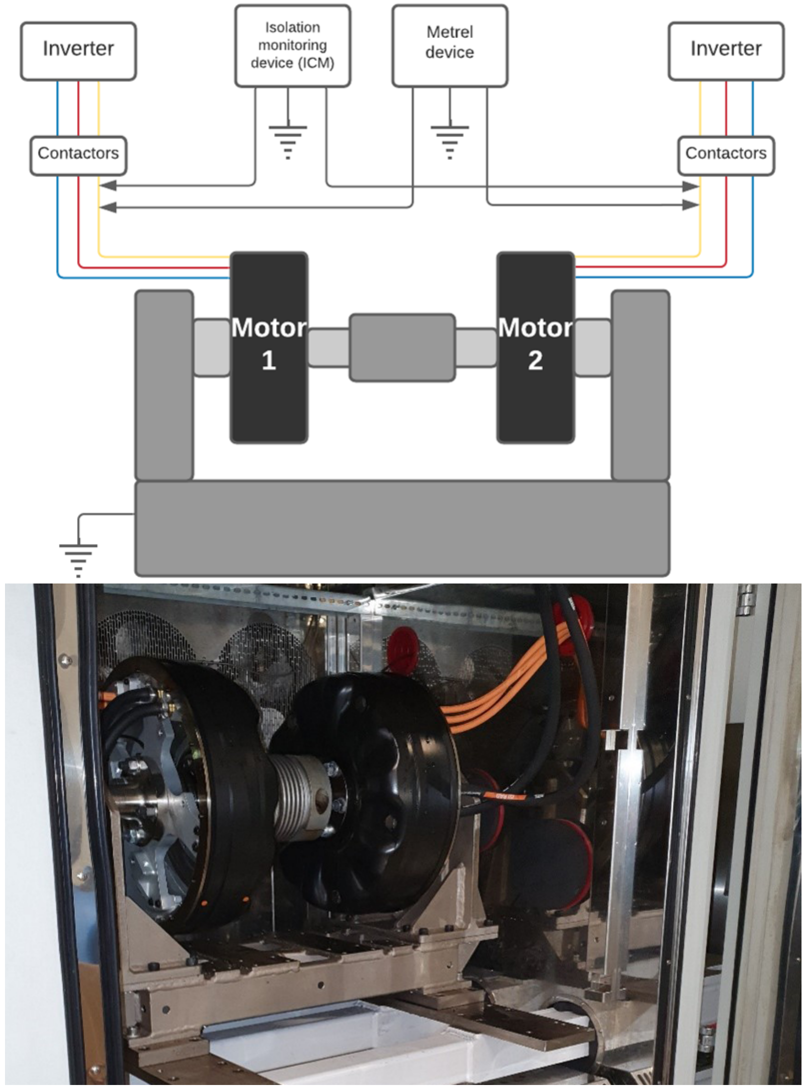

Fig. 1 An example of a test session.

4.1 Prototype Design

The basic overall design of the regression prototype consists of

- Pre-processing: Algorithms that standardize the input data and perform data linkage.

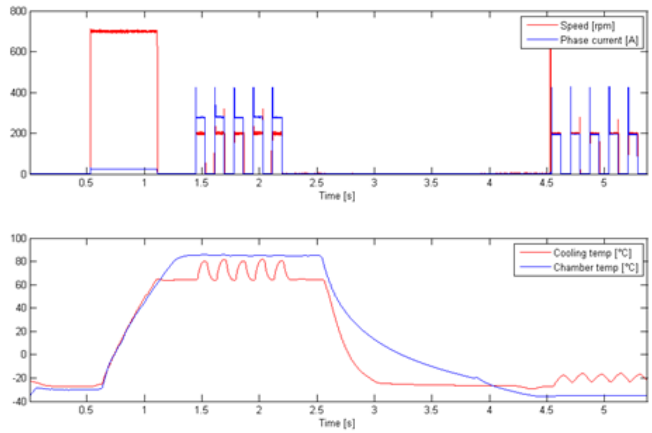

Fig. 2 Motor speed, phase current, coolant temperature, and environmental temperature within the thermal load cycle.

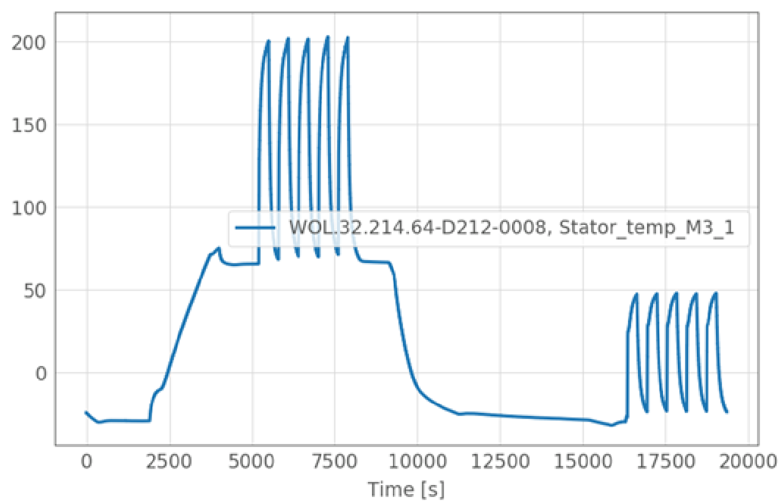

Fig. 3 Temperature profile on the motor winding during the thermal load cycle.

- Learning regression model: Machine learning regression model trained on Metrel and ICM measurements, using ICM measurements as features and Metrel resistance measurements as targets.
- Regression model: A model that is able to predict the value of the Metrel resistance measurement from ICM measurements.

Fig. 6 illustrates the aforementioned prototype.

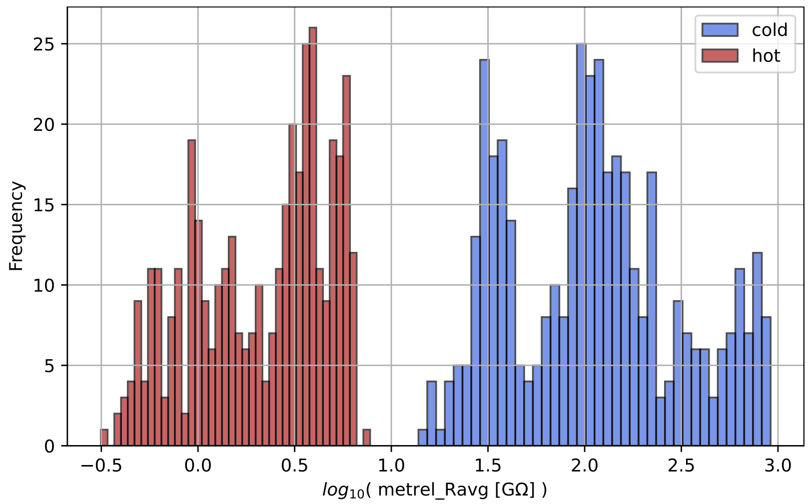

Fig. 4 Distributions of *metrel Ravg [GOhm]* during cold and hot cycles are presented (owing to the fat-tailed nature of the distributions, a logarithmic representation of resistance is shown)

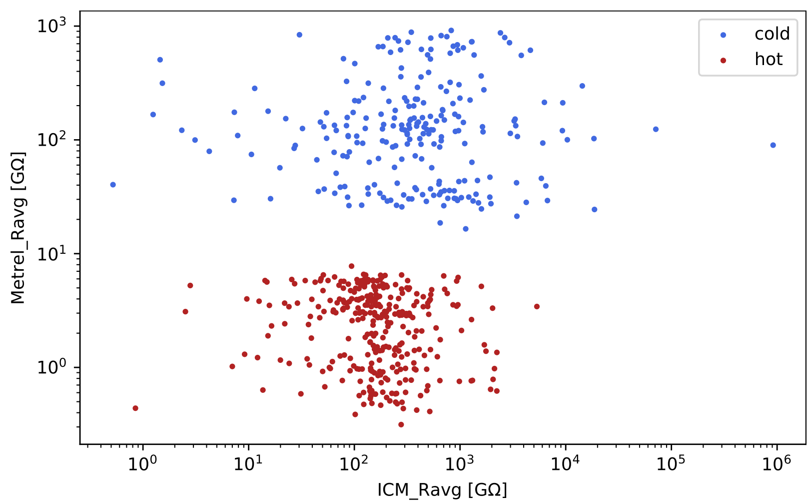

Fig. 5 Illustration of the variability and lack of association between average resistance measurements taken by ICM and Metrel.

4.2 Tested Predictive Algorithms

We use the following models to predict ICM measurements to Metrel measurements:

- *Random Forest (RF)* [7]: An ensemble learning technique that constructs multiple simpler decision trees using the bagging approach [8].

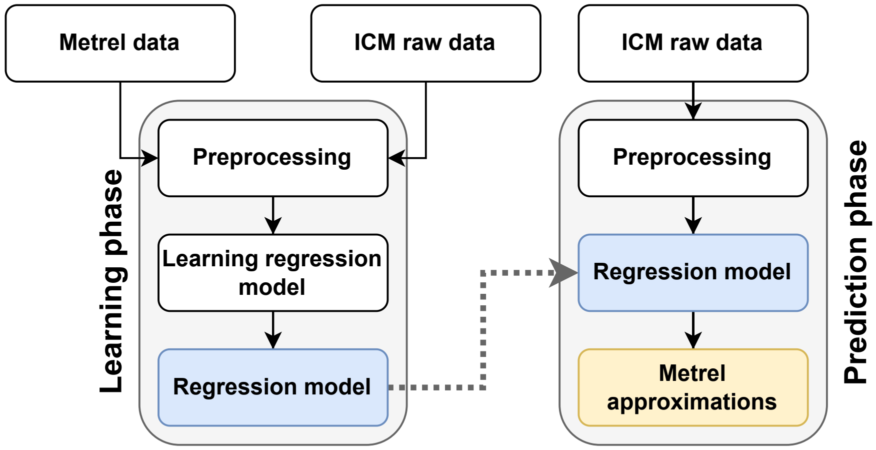

Fig. 6 Diagram of the basic design of the regression prototype.

- *Extreme Gradient Boosting (XGBoost)* [9]: This model combines numerous weak learners, especially trees that predict slightly above random. It is trained with an extended gradient boosting technique [10].
- *Mean Prediction*: A baseline strategy where all predictions are based on the mean value of the training dataset.

Both the RF and XGBoost models are a popular choice for tabular regression scenarios, especially when there is a lack of training samples [11, 12].

Feature permutation is a technique used to determine the importance of individual features in prediction models. In this method, the importance of a feature is assessed by randomly shuffling its values and observing the subsequent change in the model's performance [13]. A substantial decrease in model accuracy after shuffling indicates that the feature is important for the model's predictions. While this approach provides insights into the relationship between the model and its features, it also has its limitations. For example, it cannot accurately estimate the importance of features that are correlated with each other and its results may be affected by the model's loss function [14].

5 Experimental environment

All experiments were performed with Python v3.10. The RandomForestRegressor from the sklearn library was used for the Random Forest method, while the DummyRegressor was used for the mean approach. For Extreme Gradient Boosting we used the xgboost library. No tuning was performed and the default settings were kept for all methods. The hyperparameters can be found in table 4

Table 4 Hyperparameters used when training prediction models

Model	Parameter	Value
Random forest	number of trees	100
	bootstrap	true
	max depth	unlimited
XGBoost	learning rate	0.3
	max depth	6

The data show clear differences in resistance and temperature between hot and cold phases. To understand these differences, we conducted three experiments. The first used only data from the cold cycle, the second only data from the hot cycle and the third combined both. To test the effectiveness of each approach, we used a k-fold cross-validation in which the data were divided into k random groups. In our tests, we used $k = 10$. Using this method, we obtained k different training and validation sets, using one group for validation and the others for training. We then averaged the prediction performance from all folds to compare the approaches. Similarly, we averaged the feature importance values from the validation set across all 10 foldings.

5.1 Predictive performance results

This section evaluates the effectiveness of different regression models in estimating METREL resistance using ICM measurements. The tests were performed in both the hot and cold chamber settings. Therefore, we evaluated the models using data from the cold and hot cycle consisting of 201 and 210 data points, respectively. In the final step, we combined the data from both cycles and attempted to represent them with a unified regression model.

5.1.1 Cold cycles

First, we present the performance of the regression models during the motor's cold cycle. In Figure 7 we show the results of the selected regression models. It can be seen from the data that outliers can lead to significant deviations in the prediction errors in the different folds. Among all models, the Random Forest performs best. The crucial features are listed in Table 5. In terms of feature importance, temperature and humidity turn out to be the most important factors influencing the performance of the best model, which in this case is the Random Forest.

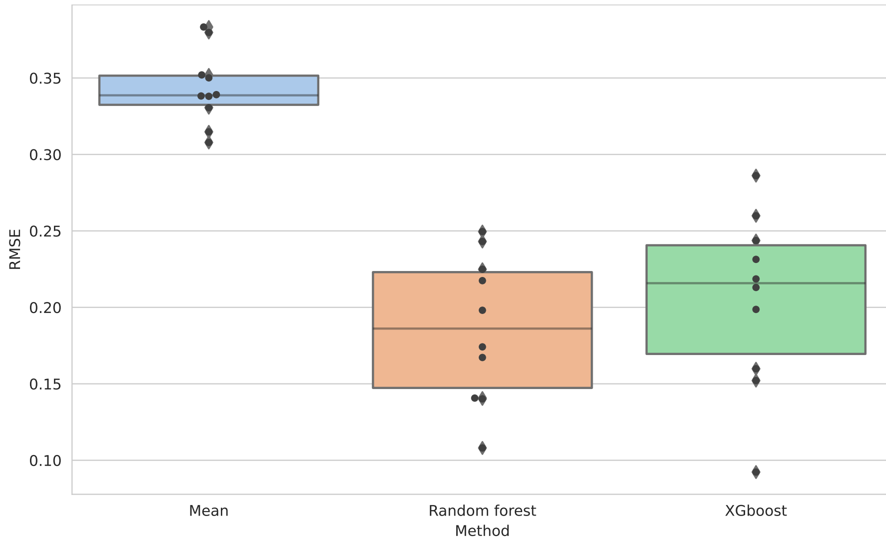

Fig. 7 RMSE prediction errors of the machine learning models for the cold cycle across all folds.

Table 5 Feature importance determined using permutation-based importance in a Random Forest model trained on data from cold cycles.

Feature name	Importance
icm_Motor temperature	0.472118
icm_Chamber humidity	0.1926
icm_Chamber temperature	0.11528
icm_Capacitance [nF] 2 Hz	0.040178
icm_Capacitance [nF] 1.5 Hz	0.030252
icm_Dissipation factor 1.5 Hz	0.018194
icm_Resistance[MOhm] 1 Hz	0.004818
icm_Resistance[MOhm] 1.5 Hz	0.00386
icm_Dissipation factor 2 Hz	0.000296
icm_Resistance[MOhm] 2 Hz	-0.000296
icm_Dissipation factor 1 Hz	-0.004851
icm_Capacitance [nF] 1 Hz	-0.004939

5.1.2 Hot cycles

Figure 8 illustrates the performance of selected regression models when the motor is in a hot cycle. We find that the prediction errors vary significantly between folds due to outliers. When comparing the models, the Random Forest consistently proves to be the best performing model. These results suggest that the Random Forest is the best fit for predicting resistance across all three scenarios.

Table 6 emphasizes the importance of the various features. When evaluating the importance of the features, temperature and humidity stand out as the most important factors for the prediction. Unlike the model based on the cold cycle data, the order of importance of chamber and motor temperature has shifted. Although we cannot definitively explain this phenomenon, our hypothesis is that the temperature within the insulation, which may lie between the chamber and motor temperatures, is central to the behavior of the model. During cold cycles, this insulation temperature seems to correlate more with the motor temperature. In hot cycles, however, it seems to be more related to the chamber temperature. This finding is consistent with our understanding of heat transfer in each scenario.

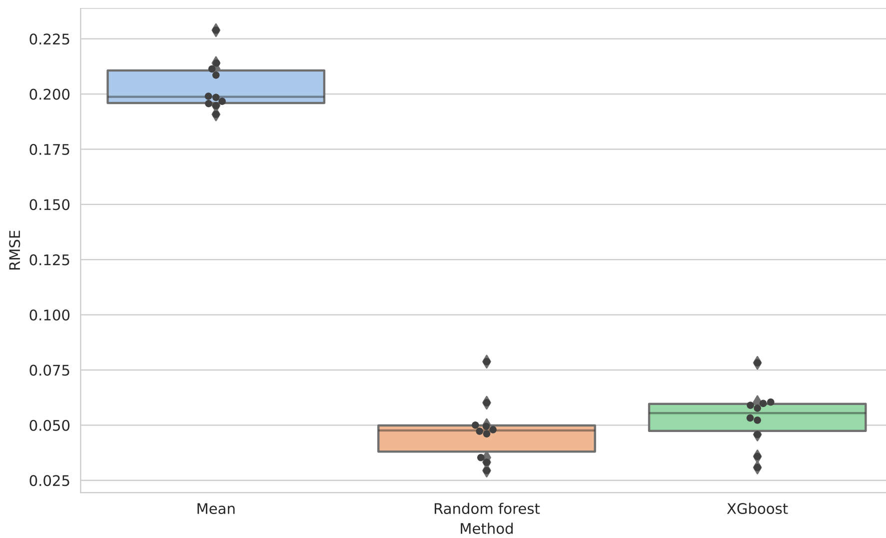

Fig. 8 RMSE prediction errors of the machine learning models for the hot cycle across all folds.

Table 6 Feature importance determined using permutation-based importance in a Random Forest model trained on data from hot cycles.

Feature name	Importance
icm_Chamber temperature	1.546679
icm_Chamber humidity	0.065118
icm_Motor temperature	0.024514
icm_Resistance[MOhm] 1 Hz	0.002612
icm_Capacitance [nF] 2 Hz	0.002359
icm_Capacitance [nF] 1 Hz	0.001196
icm_Dissipation factor 1 Hz	0.001026
icm_Resistance[MOhm] 1.5 Hz	0.000838
icm_Capacitance [nF] 1.5 Hz	0.000194
icm_Dissipation factor 1.5 Hz	-0.000012
icm_Resistance[MOhm] 2 Hz	-0.000345
icm_Dissipation factor 2 Hz	-0.000519

5.1.3 Combined cold and hot cycles

Finally, we present the performance of the regression models across all combined cycles. Figure 9 shows the results for the selected regression models. It is evident that outliers have a smaller impact on the prediction errors across different foldings. When comparing the models, the random forest and XGBoost models show comparable average performance, but the random forest appears to be more resilient.

Table 7 shows the significance of the features for cold and hot cycles together combined. Once again, temperature and humidity prove to be the most influential features for the performance of the Random Forest model. Remarkably, humidity now takes first place. As this ranking is somewhat surprising, further research with a larger data set is needed to either confirm or refute these findings.

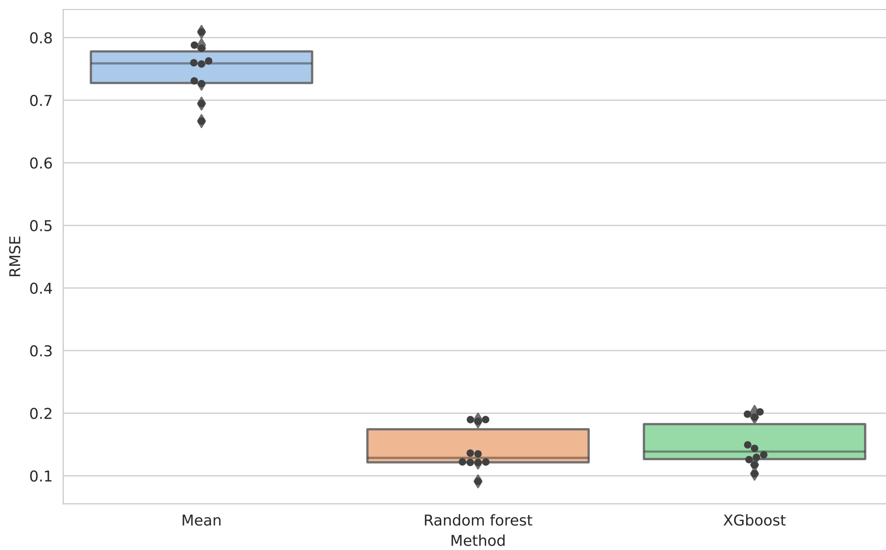

Fig. 9 RMSE prediction errors of the machine learning models for the cold and hot cycles across all folds.

6 Conclusions and Future Work

The experiment described is part of ongoing research that will be continued. A number of electric motors were tested as DUTs and several series of measurement results were collected in the harsh environment of accelerated aging, where the electric motor cycled in extreme temperature conditions under high loads. Two measurement devices were used.

Table 7 Feature importance determined using permutation-based importance in a Random Forest model trained on both hot and cold cycle data.

Feature name	Importance
icm_Chamber humidity	0.923603
icm_Motor temperature	0.138452
icm_Chamber temperature	0.074186
icm_Capacitance [nF] 2 Hz	0.010004
icm_Capacitance [nF] 1.5 Hz	0.002758
icm_Dissipation factor 1.5 Hz	0.00239
icm_Resistance[MOhm] 1 Hz	0.000856
icm_Resistance[MOhm] 1.5 Hz	0.000486
icm_Dissipation factor 1 Hz	0.000124
icm_Dissipation factor 2 Hz	0.000026
icm_Resistance[MOhm] 2 Hz	-0.000139
icm_Capacitance [nF] 1 Hz	-0.000314

The first, a commercially available device (Metrel), is considered the reference device and has a commercially specified accuracy and measurement uncertainty. It is an expensive device and as such is not suitable for use as a "mobile" device. The second is a less expensive (proprietary ICM) device that can be built in large numbers and is therefore affordable enough for use in commercially available vehicles.

The initial comparison between the two measuring devices showed little to no similarity due to the measuring resistance ranges. However, when the described AI algorithm was applied, a seemingly strong correlation was found. The random forest algorithm proved to be the most accurate and robust for this task. The correlation indicates that the measurement results obtained using only the simpler, cheaper and more mobile of the two devices tested can be used (after the AI learning phase) as a means of predicting the state of health of the electric motor insulation.

The results of the approach outlined suggest that it has the potential to support future predictive maintenance functions in electric vehicles that will be integrated into their standard equipment. This could increase the reliability of the system and the entire vehicle and make it more consistent.

For subsequent studies, it is important to collect more data from the sensors in order to validate and substantiate the findings from the preliminary data of the experiments conducted.

Future goals include extending the current research by incorporating the following enhancements:

- Monitoring and predicting the health of electric motors.
- Predicting terminal failures that can be serviced before actual failure, enabling predictive maintenance.
- Estimate the remaining lifetime of the electric motor before it needs to be replaced.

These objectives indicate the high utilization potential of the research results presented, which will contribute to increasing the value of the Elaphe company.

Acknowledgment

The authors acknowledge the financial support from the Slovenian Research Agency (research core funding No. P2-0098 and young researcher grants). The work is also part of a project that has received funding from the ECSEL Joint Undertaking under grant agreement No 876659 (iRel40).

References

1. iRel40, "Intelligent reliability 4.0," https://www.irel40.eu, 2020, accessed: 2022-04-28.
2. Elaphe, "Direct-drive in-wheel motors," https://in-wheel.com/en/solutions-2/direct-drive-in-wheel-motors/, 2019, accessed: 2022-08-04.
3. E-Mobility Engineering, "Elaphe l1500 in-wheel motor," https://www.emobility-engineering.com/elaphe-l1500-in-wheel-motor/, 2020, accessed: 2022-08-04.
4. Analog Devices, "12-bit impedance converter datasheet," https://www.analog.com/media/en/technical-documentation/data-sheets/AD5934.pdf, 2017, accessed: 2022-04-28.
5. ——, "High accuracy impedance measurements using 12-bit impedance converters," https://www.analog.com/media/en/reference-design-documentation/reference-designs/CN0217.pdf, 2013, accessed: 2022-04-28.
6. ACEA, "Wltp facts," https://www.wltpfacts.eu/, 2017, accessed: 2022-04-28.
7. T. K. Ho, "Random decision forests," in *Proceedings of 3rd international conference on document analysis and recognition*, vol. 1. IEEE, 1995, pp. 278–282.
8. L. Breiman, "Bagging predictors," *Machine learning*, vol. 24, no. 2, pp. 123–140, 1996.
9. T. Chen, T. He, M. Benesty, V. Khotilovich, Y. Tang, H. Cho, K. Chen *et al.*, "Xgboost: extreme gradient boosting," *R package version 0.4-2*, vol. 1, no. 4, pp. 1–4, 2015.
10. J. Friedman, T. Hastie, and R. Tibshirani, "Additive logistic regression: a statistical view of boosting (with discussion and a rejoinder by the authors)," *The annals of statistics*, vol. 28, no. 2, pp. 337–407, 2000.
11. R. Shwartz-Ziv and A. Armon, "Tabular data: Deep learning is not all you need," *Information Fusion*, vol. 81, pp. 84–90, 2022.
12. H. Xu, M. Ainsworth, Y.-C. Peng, M. Kusmanov, S. Panda, and J. T. Vogelstein, "When are deep networks really better than random forests at small sample sizes?" *arXiv preprint arXiv:2108.13637*, 2021.
13. A. Altmann, L. Toloşi, O. Sander, and T. Lengauer, "Permutation importance: a corrected feature importance measure," *Bioinformatics*, vol. 26, no. 10, pp. 1340–1347, 2010.
14. G. König, C. Molnar, B. Bischl, and M. Grosse-Wentrup, "Relative feature importance," in *2020 25th International Conference on Pattern Recognition (ICPR)*. IEEE, 2021, pp. 9318–9325.